# Electrooxidation of Glycerin by Potential Sweep Technique and Controlled Potential Electrolysis

*Juan Carlos Beltrán Prieto[1,*], Roman Slavík[2], Karel Kolomazník[1]*

[1] Department of Automation and Control Engineering, Faculty of Applied Informatics, Tomas Bata University in Zlín, nám. T. G. Masaryka 5555, 760 01 Zlín, Czech Republic,
[2] Department of Environmental Engineering Protection, Faculty of Technology, Tomas Bata University in Zlín, nám. T. G. Masaryka 275, 762 72 Zlín, Czech Republic
[*]E-mail: prieto@fai.utb.cz

In this study, potential sweep technique and controlled potential electrolysis were used to analyze the electrochemical oxidation of glycerin in a three electrode system using platinum as a working electrode. Electrochemical experiments were performed at different concentrations of glycerin and manganese dioxide (0.015-0.124 M) to analyze the reaction order of reactant and oxidant. Voltammograms were studied at different positive and negative potential limits (-1.5 to 1.5 V vs Ag/AgCl), sweep rates (0.01 to 0.08 V/s) and temperatures (27 to 60 °C). The influence of each parameter on the voltammogram shape is discussed. Prolonged electrolysis at controlled potential yield glyceraldehyde, glyceric acid and glycolid acid as the main products.

**Keywords:** glycerin, potential sweep, controlled potential, anodic oxidation, platinum electrode

## 1. INTRODUCTION

Large demands for biodiesel production from oils and fats generate high quantities of glycerin [1]. Excess of this byproduct requires finding nontraditional ways of its application directed towards chemicals production or generation of electricity, as an example, the application of direct glycerin fuel cells to promote C-C bond cleavage and complete oxidation into $CO_2$ [2]. Nowadays, extensively research aiming to find new applications of glycerin with special interest in the development of value added products and subsequent commercialization are intensively sought. Furthermore, the understanding of aqueous-phase heterogeneous catalysts has been essential to achieve high selectivity and yield to a particular glycerin derivative. The anodic oxidation of glycerin has been systematically investigated by several research groups. Taarning et al., studied the oxidative esterification of glycerin

catalyzed by gold nanoparticles in batch autoclave at 100 °C in 10 % sodium methoxide in methanol on both, Au/TiO$_2$ and Au/Fe$_2$O$_3$ metal oxide supported catalysts [3]. A series of consecutive oxidation reactions were observed. Methyl glycerate was the initial product, obtained via oxidation of glyceraldehyde hemiacetal. Further oxidation of methyl glycerate leads towards dimethyl tartronate, which preceded the formation of dimethyl mesoxalate as a final product with higher selectivity (89%) over Au/Fe$_2$O$_3$ in comparison to the use of Au/TiO$_2$.

The electrooxidation of glycerin in acid media using platinum nanoparticles supported on multi-walled carbon nanotubes was reported by Fernández et al., [4]. The studies using cyclic voltammetry suggested the existence of different electrooxidation steps. The formation of adsorbed CO and Pt-O at low and high potentials respectively favored the formation of CO$_2$.

Glycerin electrooxidation has been also studied in alkaline media, which strongly promoted the activity and selectivity towards acid products using Pd or Pt as catalyst. Zhang et al. [5], reported a comparative study of the electrocatalytical properties of Au and Pd electrodes in 1 M KOH solution. It was concluded that the activity and stability of glycerin oxidation on Au electrode as catalyst was higher than on Pd electrode at low onset potentials and with high peak current density. Song et al., (2012) reported the use of Au hollow spheres (Au HS) and Au/C in alkaline medium as electrocatalysts for glycerin oxidation in which Au HS demonstrated to be better catalyst [6]. In a work by Zhiani et al., [7] the catalytic activity of bis (dibenzylidene acetone) palladium catalyst, Pd(DBA)$_2$, towards glycerin oxidation was evaluated using cyclic voltammetry, electrochemical impedance spectroscopy and chronoamperometry. The studies by cyclic voltammetry suggested the oxidation of freshly chemisorbed species from glycerin adsorption in the forward scan and the removal of not oxidized carbonaceous species in the reverse scan. The catalyst demonstrated to have high tolerance and stability as it was active even after 200 cycles. Studies using chronoamperometry revealed current decay which was associated to the adsorption of glycerin derivatives on surface catalyst. The analysis by electrochemical impedance spectroscopy indicated the presence of byproducts and intermediates that poisoned the catalyst surface after 200 cycles. The synthesis of dihydroxyacetone has been also reported by Rodrigues et al., [8] using gold nanoparticles supported on multi-walled carbon nanotubes in alkaline media (NaOH) with high selectivity and activity due to the metal-support interaction and specific adsorption properties.

Several authors have emphasize the complexity and difficulty of anodic oxidation of small organic compounds [9,10] particularly on understanding the oxidation mechanism, which is caused by the presence of adsorbed intermediates and electronic bonds between the adsorbate and the surface of the noble metal. Moreover, it has been proved that the activity towards glycerin oxidation is strongly affected by the presence of intermediates [10]. The challenge of glycerin oxidation lays on the selection of an environmentally friendly oxidation method that leads towards desired products at acceptable yield and selectivity for potential industrial application. The oxidation of benzylic and allylic alcohols towards aldehydes and ketones in presence of MnO$_2$ and O$_2$ was recently studied by Kamimura [11]. Although several efforts have been made to oxidize primary and secondary alcohols to aldehyde and ketones using MnO$_2$ without further overoxidation to carboxylic acids, only a few papers have been discussed aiming to selectively oxidize glycerin to glyceraldehyde.

In the present study, the anodic oxidation of glycerin on platinum electrode in presence of a metal oxidant was investigated using potential sweep technique and controlled potential electrolysis. These electrochemical procedures allow the analysis of the potential effect on current density and the potential regulation during the partial anodic oxidation of glycerin.

## 2. METHODOLOGY

### 2.1. Chemicals and Reagents

Deionized water was used in all procedures (Millipore). Glycerin (Propane-1,2,3-triol) and manganese dioxide ($MnO_2$) were obtained from Sigma-Aldrich (Czech Republic).

### 2.2. Voltammetric Measurements

Electrochemical experiments were performed in a three electrode glass cell of 25 mL capacity. The partial oxidation of glycerin was analyzed using a three electrode system. A Pt electrode was used as working electrode. Silver/silver chloride electrode was the reference electrode and boron-doped diamond as auxiliary electrode. The glycerin electrooxidation reaction was studied in presence of $MnO_2$. Potential sweep technique was used systematically in the present work. Three different cyclic voltammogram analyses were performed in the presence and absence of glycerin and $MnO_2$ at the same scan rate (50 mV/s) and room temperature within a potential range of -1.5 and 1.5 V vs Ag/AgCl to study the dependence of the current on an applied triangular potential-time waveform as showed in Figure 1. The first voltammogram was obtained using a 0.014 M $MnO_2$, the second one in 0.06 M glycerin and the third one using 0.014 M $MnO_2$. The potentials reported are all referred to Ag/AgCl electrode
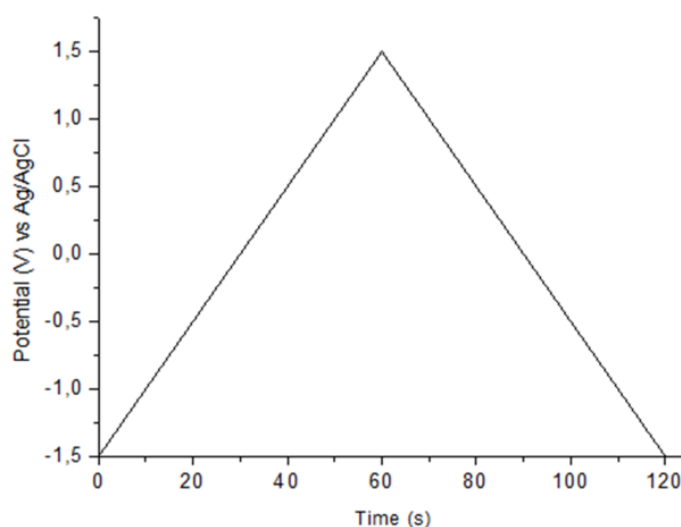


**Figure 1.** Symmetrical waveform of the potential sweep technique.

## 2.3. Effect of varying glycerin and MnO$_2$ concentration

Data from electroanalytical measurements were analyzed using PSTrace software. In order to analyze the reaction order for glycerin and MnO$_2$ two different cyclic voltammogram analyses were performed at 50 mV·s$^{-1}$ in a potential range of -1.5 to 1.5 V vs Ag/AgCl. The first group of voltammograms consisted in 0.06 M glycerin solutions with MnO$_2$ concentration between 0.015 and 0.124 M, while the second group was realized in the presence of 0.014 M MnO$_2$ and glycerin concentration in a range of 0.015-0.124 M.

## 2.4. Effect of potential scan limits, scan rate and analysis of temperature variation

The effect of the increment of positive and negative potential limit was studied in a range of -1.5 to 1.5 V vs Ag/AgCl for solutions of 0.06 M glycerin in 0.014 M MnO$_2$. Cyclic voltammograms were recorded at a scan rate of 0.05 V·s$^{-1}$ and 25 °C. A scan rate of 0.01 to 0.08 V·s$^{-1}$ was studied in 0.06 M glycerin in presence of 0.014 M MnO$_2$. For the analysis of temperature effect, similar parameters were employed using a scan rate of 0.03 V·s$^{-1}$ in a temperature range of 27 to 60 °C.

## 2.5. Controlled potential electrolysis

Controlled potential electrolysis was used during prolonged oxidation reaction to analyze the glycerin derivatives formed and to test the influence of MnO$_2$ towards glyceraldehyde production. The oxidation of 8 mM glycerin in presence of 0.24 mM MnO$_2$ was performed at 1.05 V vs Ag/AgCl over a 4 h period time. The quantitative analysis of these samples was carried out by High Performance Liquid Chromatography (HPLC). The chromatographic method used for the analysis of glycerin derivatives is described in a previous paper [12].

# 3. RESULTS

## 3.1. Analysis of cyclic voltammetric data

Figure 2 describes the cyclic voltammogram of Pt electrode in the presence and absence of MnO$_2$ and glycerin. It can be seen that in all cases hydrogen evolution takes place (hydrogen adsorption and desorption) at negative potentials. In a), hydrogen evolution occurs between -1 and -0.25 V vs Ag/AgCl in the forward scan, while the positive charge in the reversed scan corresponds to the oxidation of the hydrogen. When using the oxidant alone, a non-Faradaic current was observed. However, in the presence of reagent and oxidant, with the onset of the electrooxidation reaction, there was a charge transferred across the electrified interface and the Faradaic current flow increased rapidly until, at different particular potentials, a maximum current or peak current was observed followed by a subsequent decrement of current. When the direction of the applied potential is reversed in the cathodic direction the current decreases until the product of the electrooxidation reaction is reduced at

the electrode surface at a particular potential. This step is characterized by a current increment until a maximum cathodic current was reached. After, the current decreased until the cycle is completed and the direction of the applied potential is reversed. The adsorption of OH^{-} and formation of PtOH[-] occurs at -0.1 V vs Ag/AgCl, followed by a surface oxidation process such as the conversion of PtOH to form platinum oxide at 0.6 V vs Ag/AgCl. The reduction of platinum oxide is shown in the reversed scan at 0.11 V vs Ag/AgCl, followed by the oxidation of glycerin at 0.07 V vs Ag/AgCl and hydrogen desorption. As suggested by Roquet et al., glycerin oxidation requires the presence of adsorbed OH^{-} groups at the platinum surface [13].
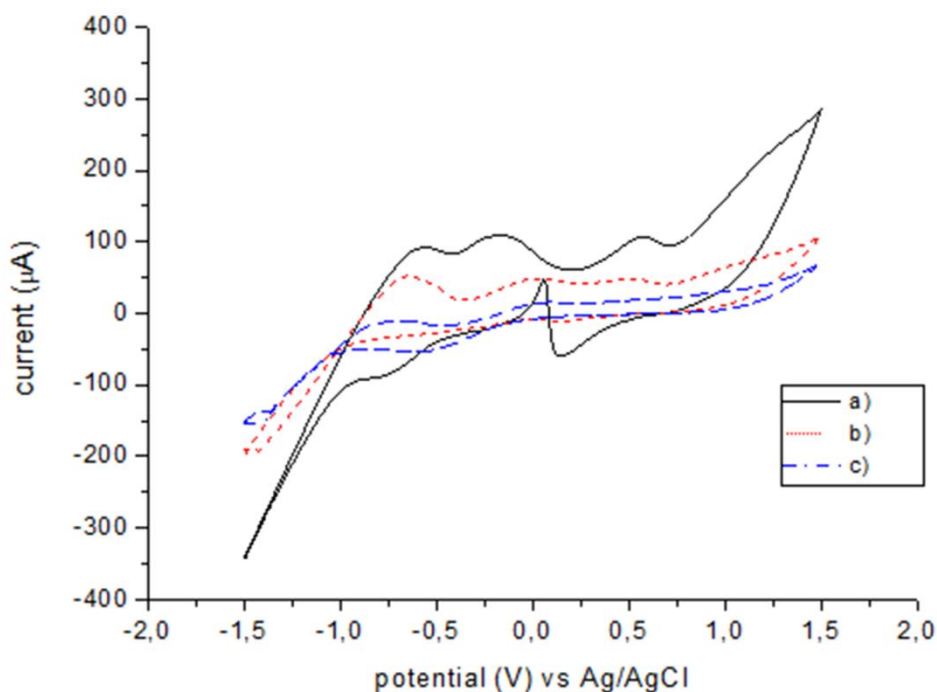


**Figure 2.** Cyclic voltammogram analysis of Pt electrode at 50 mV·s^{-1} in the presence  a) 0.014M $MnO_2$ + 0.125 M glycerin; b), 0.06 M glycerin c) 0.014 M $MnO_2$

*3.2. The analysis of glycerin and $MnO_2$ reaction order*

The order of the reaction with respect to glycerin and $MnO_2$ is the observed dependence of the reaction rate on the concentration of the specific reactant when the concentrations of all other species in the reaction are constant. To calculate the reaction order of glycerin, a cyclic voltammetry study was performed in 0.014 M $MnO_2$ and variation of the reagent concentration from 0.015-0.125 M. Equation (1) was used to calculate the reaction order at specific potentials by means of the analysis of the anodic current at the corresponding concentration.

$$r = (\partial \log I / \partial \log [C_3 H_8 O_3]) \tag{1}$$

Figure 3 shows the plot of log current density vs log glycerin concentration for the three peaks. For peaks at -0.7 (peak I) and -0.2 V(peak II), no reaction order could be obtained over the range of concentrations studied indicating that the oxidation was inhibited by the reagent concentration due to saturation of active sites and preventing the OH^{-} adsorption on Pt surface. However, under the

consideration of lower glycerin concentrations (< 0.033 M) it was possible to obtain a reaction order for both peaks, corresponding to 0.6 and 0.3 respectively. Peak at 0.6 V (peak III) presented a slope of 0.22. The fractional values demonstrate the complexity of the reaction mechanism and that the rate determining step involves adsorbed species generated during the oxidation [14].
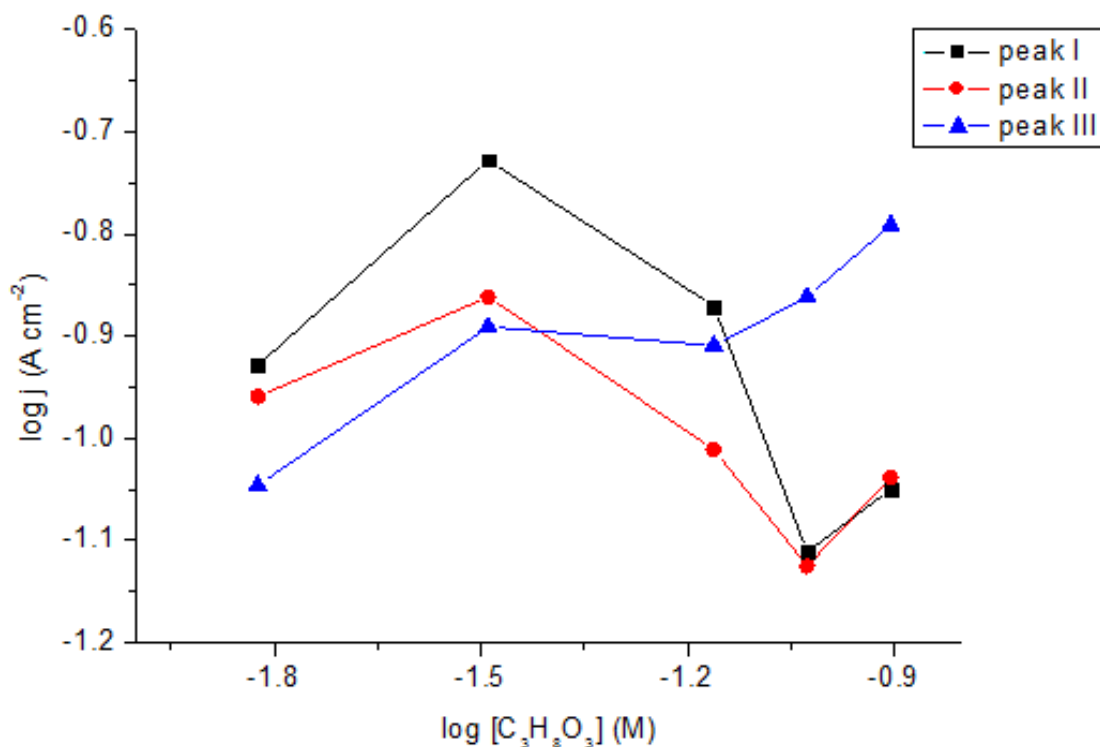


**Figure 3.** Analysis of the variation of glycerin concentration on the current density (j) at different potentials for glycerin solutions (0.015-0.125 M) in 0.014M $MnO_2$.

For the analysis of $MnO_2$ reaction order, equation (2) was taken into account:

$$r' = (\partial \log I / \partial \log[MnO_2]) \qquad (2)$$

When varying the concentration of $MnO_2$ between 0.015 and 0.125 M and keeping constant the concentration of glycerin (0.06 M), an slope of r'=-0.61, 0.44 and 0.22 for each different peaks (Figure 4). The negative sign is related to inhibition of glycerin oxidation by increasing of $OH^-$ in the media. Increment of $MnO_2$ concentration shifted the peak to more positive potentials. It is likely that the decreasing in current is due to oversaturation of $OH^-$ and adsorbed intermediates which prevent the glycerin adsorption on Pt sites.

The analysis of kinetic parameters suggests the presence of a reversible electron transfer with adsorption-diffusion coupling and with a partial reaction order presented in Table 1.
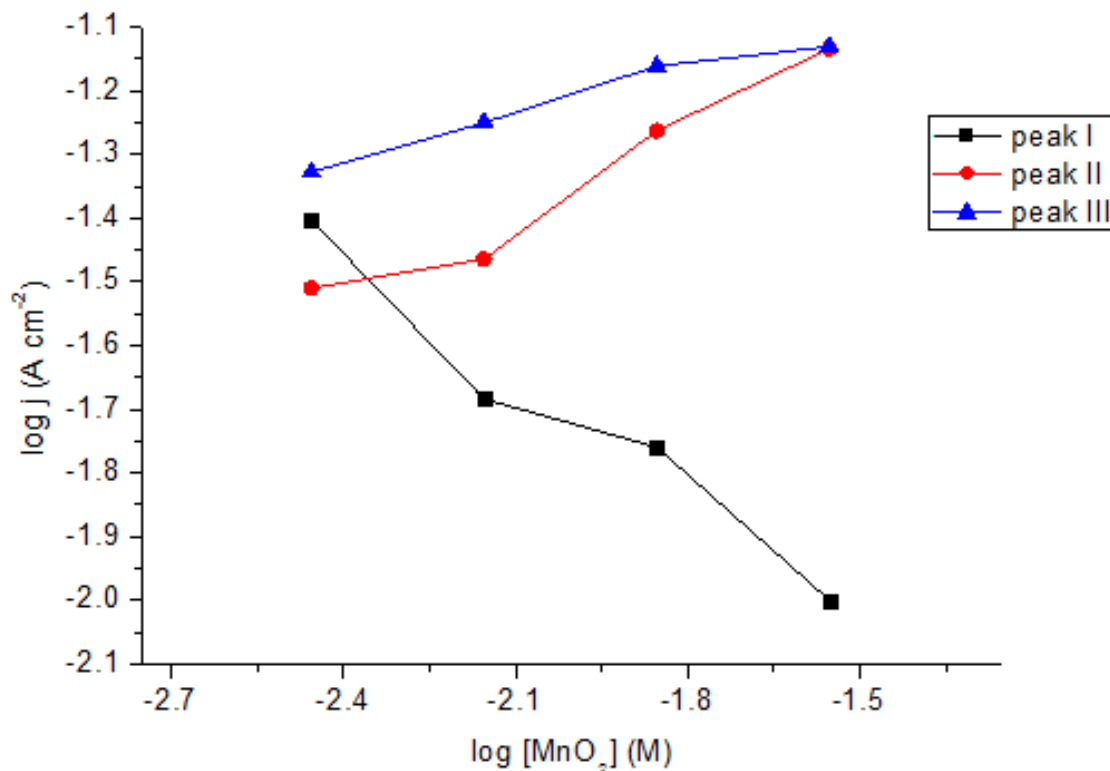
**Figure 4.** Log of peak current vs log of oxidant concentration for partial oxidation of glycerin.

**Table 1.** Reaction order with respect to glycerin and $MnO_2$ for the electrooxidation of glycerin

| E (V) vs Ag/AgCl | r $C_3H_8O_3$ | r' $MnO_2$ | Expression for the rate of the determining step. |
|---|---|---|---|
| -0.7 | 0.6 | -0.61 | $v = k[MnO_2]^{-0.61}[C_3H_8O_3]^{0.6}e^{(nFE/RT)}$ |
| 0.2 | 0.48 | 0.44 | $v = k[MnO_2]^{0.44}[C_3H_8O_3]^{0.48}e^{(nFE/RT)}$ |
| 0.6 | 0.22 | 0.22 | $v = k[MnO_2]^{0.22}[C_3H_8O_3]^{0.22}e^{(nFE/RT)}$ |

*3.3. The effect of potential scan limits on cyclic voltammogram*

The variation of positive potential limits of scan are presented on Figure 5, in a range of -1.5 to 1.5 V vs Ag/AgCl using solutions of 0.06 M glycerin in 0.014 M $MnO_2$ by cyclic voltammetry in platinum electrode at a scan rate of 0.05 V/s and room temperature. It is clearly seen that the increase in potential caused a slightly decrease in the peak current at -0.7 V during the anodic sweep. This might indicate that adsorbed glycerin or intermediates are blocking the surface of the platinum electrode.
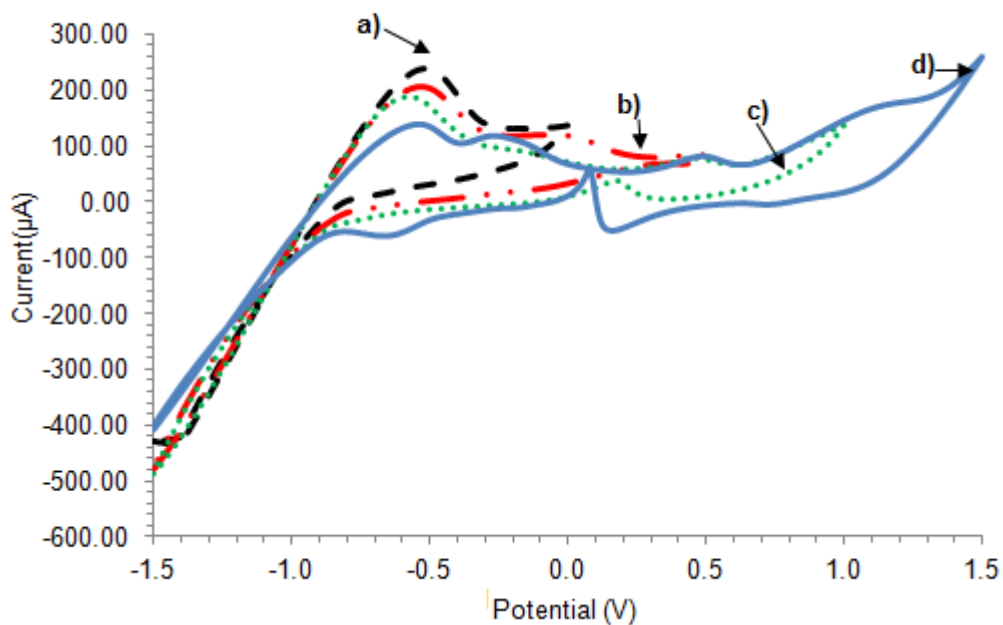
**Figure 5.** Cyclic voltammogram for glycerin oxidation varying forward potential limit. a) 0 V, b)0.5 V, c) 1 V, e) 1.5 V in 0.06 M glycerin + 0.014 M $MnO_2$ (25 °C, 0.05 V/s).

When the scan limit is 1.5 V vs Ag/AgCl, there is a postwave at -0.235 V vs Ag/AgCl indicating the oxidation of strongly adsorbed reactant. A comparison using a potential limit of 1.3 V vs Ag/AgCl (Figure 6) clearly shows that the peak on the negative potential is not affected by the adsorption of the reactant. At lower positive potential limits the reactant is weakly adsorbed and an increase in the current of the cathodic peak is observed due to the contribution of both, adsorbed and diffusing glycerin. The enhancement of the current peak in the reverse scan shows that the products are weakly adsorbed.
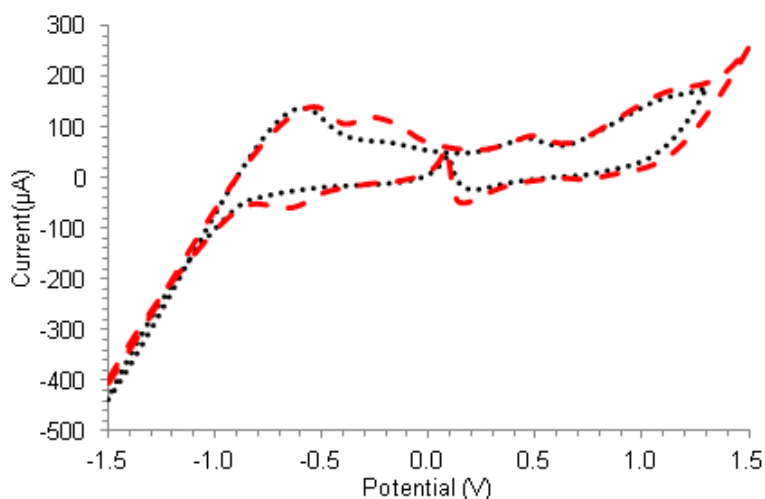


**Figure 6.** Cyclic voltammogram for glycerin oxidation varying forward potential limit. (dotted line - 1.5 to 1.3 V; dashed line (---) -1.5 to 1.5 V) in 0.06 M glycerin + 0.014 M $MnO_2$ (25 °C, 0.05 V/s).

The variation of negative limit potential is presented on Figure 7. Using potentials of 0 and -0.5 V vs Ag/AgCl showed no oxidation or reduction peaks. Therefore, the oxidation started at more negative potentials. Increasing the negative potential limit enhanced current peaks which were shifted to more positive potentials. Since lower potential limits controls the hydrogen adsorption, as explained in [9], it can be stated that decreasing the potential did not caused an inhibition effect by possible reaction of adsorbed glycerin and the adsorbed hydrogen layer. The peak presented in the reversed scan (around 0.05-0.1V vs Ag/AgCl) using scans from -1.2 V vs Ag/AgCl arose from the reduction of oxides and glycerin oxidation [15]. The increment on the current of the reverse scan peaks confirmed that the product was weakly adsorbed.
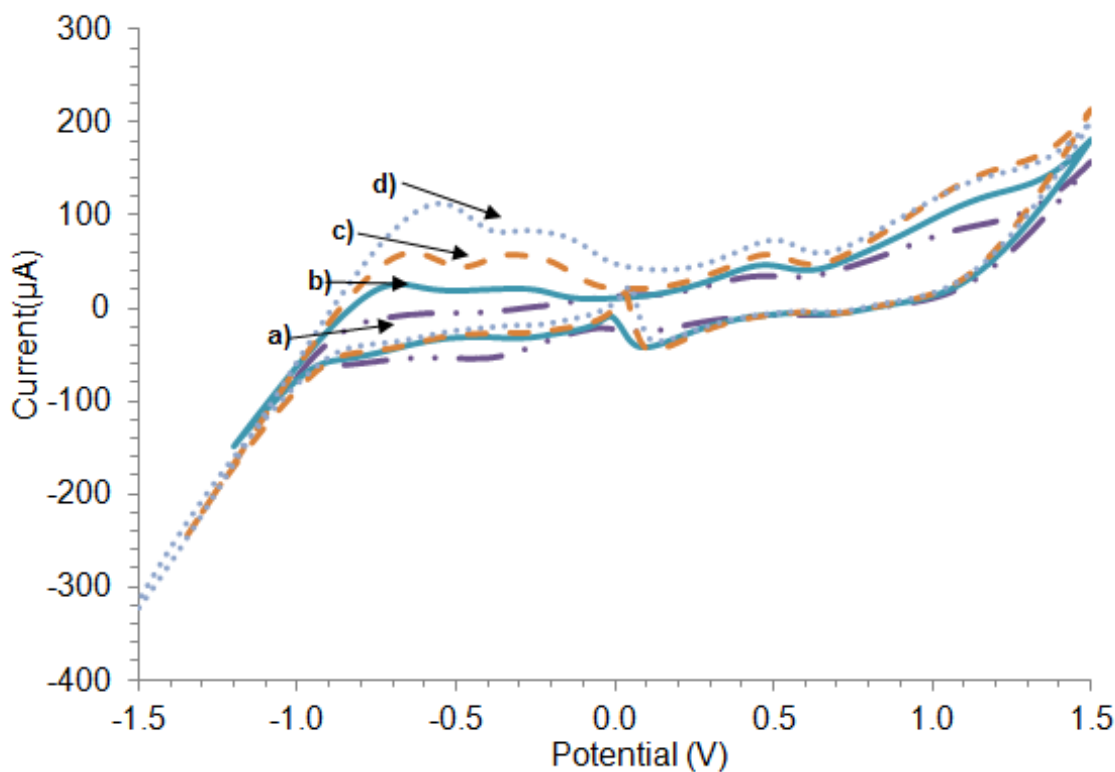


**Figure 7.** The effect of varying the negative potential limit on cyclic voltammograms at 25 °C and 0.05 V/s. a) -1 V, b) -1.2 V, c) -1.35, d) -1.5 V.

*3.4. The effect of sweep rate variation on cyclic voltammogram*

The variation of sweep rate was studied from 0.01 to 0.08 V/s in 0.06 M + 0.014 M $MnO_2$. The dependence of the peak potential and variation of sweep rate is presented in Figure 8. The potential for the peak at -0.7 V was shifted slightly to more negative potentials at higher sweep rates, while the other peaks were shifted to more positive potentials (Figure 9).
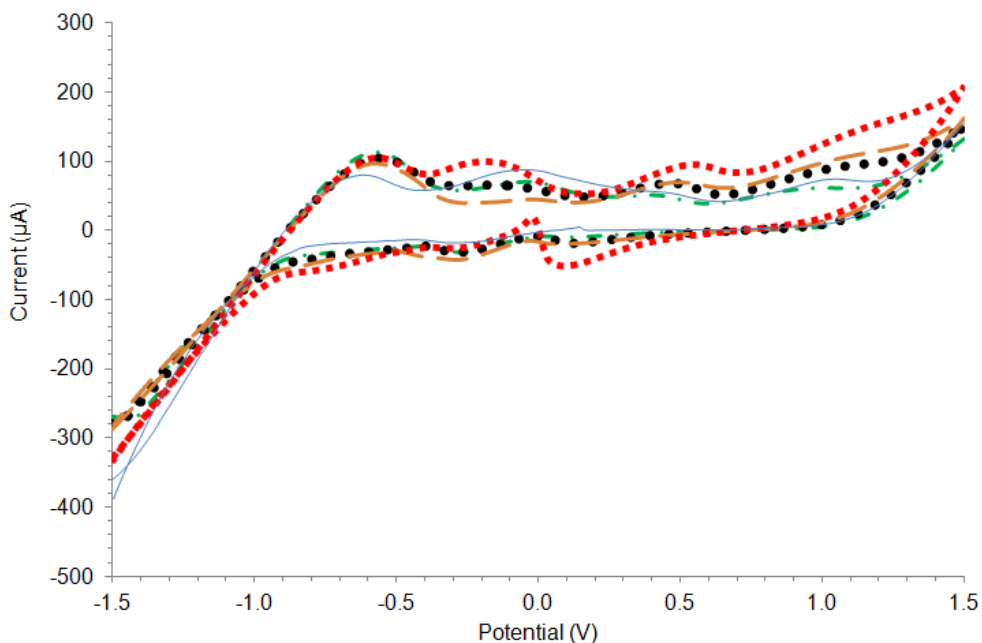
**Figure 8.** Effect of varying the sweep rate on the voltammograms of a platinum electrode in 0.06 M glycerin + 0.014 M $MnO_2$ (25 °C). Solid line: 0.01 $V \cdot s^{-1}$; dash dot line: 0.03 $V \cdot s^{-1}$; round dot line: 0.05 $V \cdot s^{-1}$; long dash line: 0.07 $V \cdot s^{-1}$; square dot line: 0.1 $V \cdot s^{-1}$.
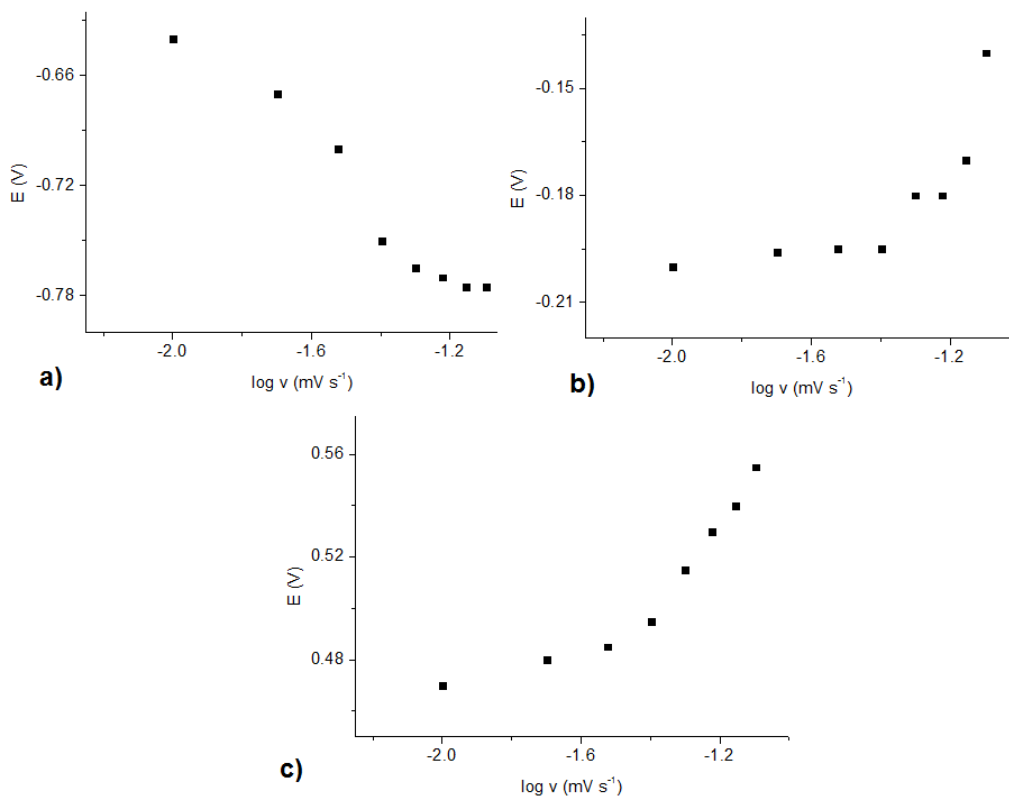


**Figure 9.** Plot of peak potential against the logarithm of sweep rate for platinum electrode in 0.06 M glycerin + 0.014 M $MnO_2$ (25 °C). a) Peak at -0.7 V, b) Peak at -0.2 V, c)Peak at 0.6 V.

The degree of kinetic reversibility is function of the sweep rate. It is expected that a reaction that is surface-transport-controlled is characterized by a non-variation of peak potential at small sweep rates and a linear variation of peak potential at higher sweep rates [16]. The linear dependence of the anodic peak current on the corresponding square root of the scan rate showed that the oxidation process is surface-transport-controlled (Figure 10). However, the fact that a linear relationship was also obtained for a peak current vs sweep rate plot (Figure 11) suggests that the redox compound is also adsorbed on the electrode surface.
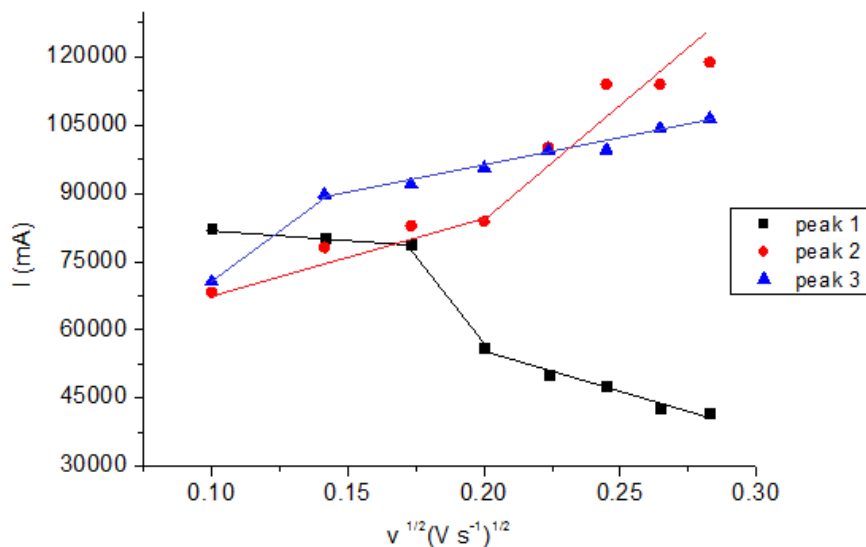


**Figure 10.** Dependence on anodic peak current on the applied scan rate obtained from cyclic voltammetry
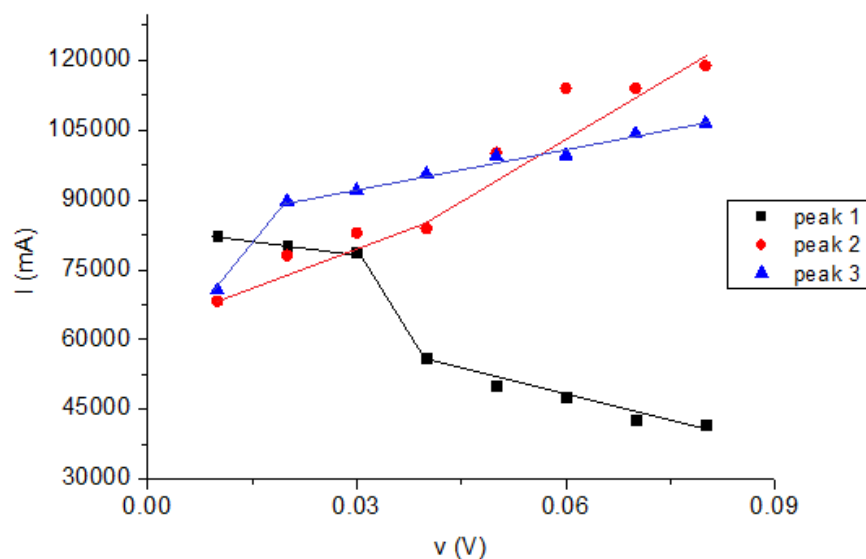


**Figure 11.** Plot of current peak against sweep rate potential that shows the possibility of adsorbed species.

*3.5. The effect of temperature on cyclic voltammogram*

The variation of temperature in the range of 27 to 60 °C showed that the anodic current increased at higher temperatures. In addition, peaks at -0.7 V and -0.2 V were shifted to more negative potentials. At 27°C, these were found at -0.7, and -0.2 V vs Ag/AgCl respectively and at 60 °C, they appeared at -0.76 and -0.35 V vs Ag/AgCl. The determination of the apparent activation energy ($\Delta E^*$) was performed from the slope values obtained in the plots of log $j$ vs. $T^{-1}$ in the temperature range under study for the first and third peak and below 40 °C for the second peak. The values were obtained from the linear regression and are presented in Table 2. Arrhenius plots for glycerin oxidation are presented in Figure 12.
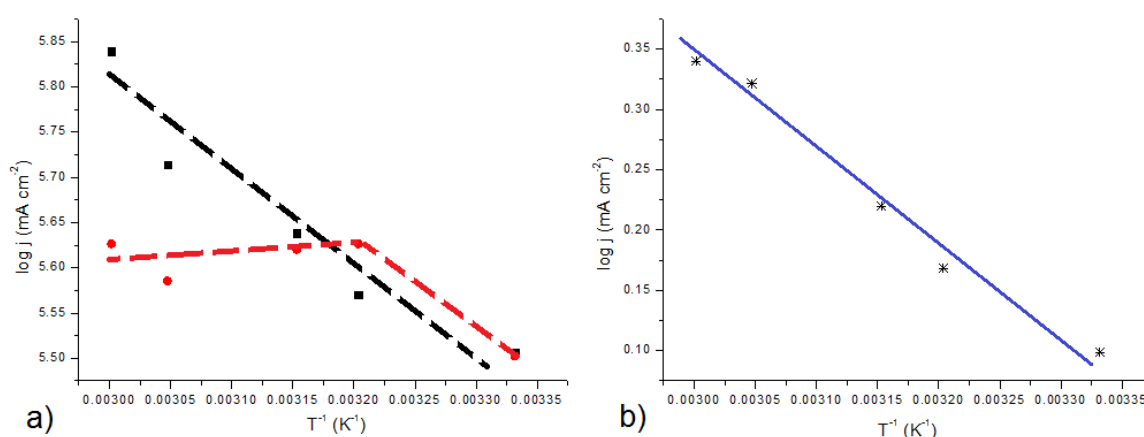


**Figure 12.** Arrhenius plot for glycerin oxidation. (■) peak I (at -0.7 V); (●) peak II (at -0.2 V); (*) peak III (at 0.6 V).

**Table 2.** Apparent activation energy ($\Delta E^*$) for the forward scan peaks detected.

| Peak | E (V)[a] vs Ag/AgCl | $\Delta E^*$ (kJ mol$^{-1}$) |
|------|---------------------|------------------------------|
| I    | -0.76               | 6.19                         |
| II   | -0.35               | 7.48                         |
| III  | 0.8                 | 6.52                         |

[a] average of the peak potential at different temperatures

*3.6 Oxidation of glycerin using controlled potential electrolysis*

Controlled potential electrolysis was used to evaluate the production of glyceraldehyde using Pt electrode in presence of $MnO_2$. The products formed were identified and quantified by means of HPLC. The three main products generated during the first 4 hours of reaction were glyceraldehyde (40 % selectivity), glyceric acid (24 % selectivity), and glycolic acid (4.23 % selectivity). Studies performed by Henbest and Thomas (1957) reported that the activity of manganese dioxide depends on several aspects, such as the substrate used, the availability of oxygen in the oxidant and to the fact that

it acts as a non-stoichiometric compound [17,18]. Moreover, Lai et al., [19] reported that the presence of low electron density sites in the molecule of manganese dioxide is strongly related to the selectivity towards the aldehyde.

## 4. CONCLUSION

In the present research, potential sweep technique and controlled potential electrolysis were used to evaluate the electrochemical oxidation of glycerin on platinum to get a better understanding of the electrocatalytic reaction. The plot of anodic peak currents versus the square root of scan rates showed a strongly linear proportion, which is expected for diffusion controlled electrode process. The controlled potential electrolysis led to the oxidation of the primary carbon atom of the glycerin molecule, allowing the formation of derivatives with aldehyde and carboxylic acids groups. Among the several products obtained, glyceraldehyde was the product that presented the higher selectivity.

**References.**

1.  M. Hunsom and P. Saila, *Int. J. Electrochem. Sci.* 8 (2013) 11288.
2.  R. L. Arechederra and S. D. Minteer, *Fuel Cells* 9 (2009) 63.
3.  E. Taarning, A. Madsen, and J. Marchetti, *Green Chem*. 10 (2008) 408.
4.  P. S. Fernández, M. E. Martins, and G. a. Camara, *Electrochim. Acta* 66 (2012) 180.
5.  J. Zhang, Y. Liang, N. Li, Z. Li, C. Xu, and S. P. Jiang, *Electrochim. Acta* 59 (2012) 156.
6.  M. Zhiani, H. Rostami, S. Majidi, and K. Karami, *Int. J. Hydrogen Energy* 38 (2013) 5435.
7.  J. Song, S. Fan, J. Yu, K. Ye, and C. Xu, *Int. J. Electrochem. Sci*. **7** (2012) 10842.
8.  E. G. Rodrigues, M. F. R. Pereira, J. J. Delgado, X. Chen, and J. J. M. Órfão, *Catal. Commun*. 16 (2011) 64.
9.  C. Lamy, *Electrochim. Acta* 29 (1984) 1581.
10. D. Takky, B. Beden, J.-M. Leger, and C. Lamy, *J. Electroanal. Chem. Interfacial Electrochem*. 193 (1985) 159.
11. A. Kamimura, H. Komatsu, T. Moriyama, and Y. Nozaki, *Tetrahedron* 69 (2013) 5968.
12. J. C. Beltrán-Prieto, J. Pecha, V. Kašpárková, and K. Kolomazník, *J. Liq. Chromatogr. Relat. Technol.* (2013) 36, 37.
13. L. Roquet, E. M. Belgsir, J.-M. Léger, and C. Lamy, *Electrochim. Acta* 39 (1994) 2387.
14. A. Velázquez-Palenzuela, F. Centellas, J. A. Garrido, C. Arias, R. M. Rodríguez, E. Brillas, and P.-L. Cabot, *J. Power Sources* 196 (2011) 3503.
15. M. Schell, Y. Xu, and Z. Zdraveski, *J. Phys. Chem*. 100 (1996) 18962.
16. M. E. G. Lyons and G. P. Keeley, *Sensors* 6 (2006) 1791.

17.  H. B. Henbest, E. R. H. Jones, and T. C. Owen, *J. Chem. Soc*. (1955) 2765.
18.  H. B. Henbest and A. Thomas, *J. Chem. Soc*. (1957) 3032.
19.  T. K. Lai, J. Banerji, A. Chatterjee, and B. Basak, *Indian J. Chem. Sect*. B 44 (2005) 1309.